DOI: 10.1002/ejic.200500691

Manganese Azides Based on Co-Ligands with a Flexible Tail: Diverse Structural and Magnetic Properties

Shi-Qiang Bai,[a] En-Qing Gao,[a,b] Zheng He,[a] Chen-Jie Fang,[a] Yan-Feng Yue,[a] and Chun-Hua Yan*[a]

Keywords: Azides / Coordination polymers / Ligand design / Magnetic properties / Manganese

Three azido-bridged coordination polymers, namely $[Mn(L^1)(N_3)_2]_n$ (**1**), $[Mn(L^2)(N_3)_2]_n$ (**2**), and $[Mn(L^3)(N_3)_2]_n$ (**3**) [L^1 = *N*-(2-pyridylmethylene)methylamine, L^2 = *N*-(2-pyridylmethylene)ethylamine, and L^3 = *N*-(2-pyridylmethylene)octylamine], have been synthesized with Schiff-base co-ligands with flexible tails, and their structures and magnetic properties characterized. Complex **1** is composed of one-dimensional, uniform chains with double end-on (EO) azido bridges, complex **2** consists of (6,3) net layers in which double EO azido-bridged dimers are interlinked by single end-to-end (EE) azido bridges, and complex **3** contains chains of Mn^{II} ions bridged by alternating double EO and double EE azido bridges. Magnetically, **1** is a metamagnet built of ferromagnetic chains, **2** exhibits weak ferromagnetism due to spin canting, and **3** shows alternate ferro- and antiferromagnetic intrachain interactions.

Introduction

Magnetic coordination polymers have attracted intense interest due not only to fundamental research into magnetic interactions but also the need for new molecule-based materials. Their magnetic properties depend on the nature of the interacting metal ions, and can be tuned by the nature of the bridging ligand and by the whole structural arrangement.[1] In recent years, an increasing number of azidomanganese(II) coordination polymers with different co-ligands have been reported that present a remarkable diversity in bridging topology, polymeric dimensionality, and bulk magnetic properties.[2–6] The main factors causing such diversity are the extreme versatilities of the azido ligating mode in bridging metal ions and in transmitting magnetic interactions. The azido bridge transmits mainly ferromagnetic (FM) interactions for the end-on (EO) binding mode and antiferromagnetic (AFM) interactions for the end-to-end (EE) mode.

Despite the large number of manganese azide complexes, no general correlation has been found so far between the properties of the co-ligand and the coordination mode of the azido bridge. Recently, we have reported a series of azidomanganese(II) complexes with didentate Schiff bases derived from 2-pyridylaldehyde and aniline derivatives, which exhibit similar one-dimensional (1D) structures with alternating double EO and double EE azido bridges despite the different substituents on the aniline moiety.[3i] Along this line, we decided to extend this study to similar didentate Schiff bases derived from aliphatic amines to investigate the correlation between the polymeric structures and the co-ligands. Here, we report the structural and magnetic properties of three new azidomanganese(II) complexes with didentate Schiff-base co-ligands derived from methylamine, ethylamine, and octylamine (Scheme 1). As will be shown, although they have the same $[Mn(L^i)(N_3)_2]_n$ stoichiometry, the structures vary from a 1D uniform chain with double EO azido bridges {$[Mn(L^1)(N_3)_2]_n$, **1**}, through a two-dimensional (2D) layer with double EO, and single EE azido bridges {$[Mn(L^2)(N_3)_2]_n$, **2**}, to a 1D chain with alternating double EO and double EE azido bridges {$[Mn(L^3)(N_3)_2]_n$, **3**} with increasing steric demand of the co-ligands L^1, L^2, and L^3, respectively. Consequently, these complexes exhibit different magnetic properties.

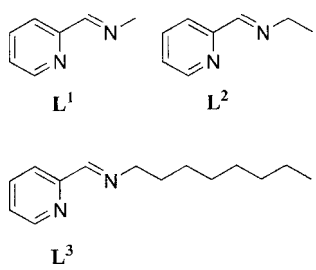

L^1 L^2

L^3

Scheme 1.

[a] State Key Lab of Rare Earth Materials Chemistry and Applications & PKU-HKU Joint Lab on Rare Earth Materials and Bioinorganic Chemistry, Peking University,
Beijing 100871, China
Fax: +86-10-6275-4179
E-mail: yan@pku.edu.cn
[b] Shanghai Key Lab of Green Chemistry and Chemical Processes, Department of Chemistry, East-China Normal University,
Shanghai 200062, China

Results and Discussion

Complex **1** was prepared as crystals by slow interdiffusion between a methanol solution containing $Mn(ClO_4)_2 \cdot 6H_2O$ and L^1 and a methanol solution of NaN_3. Crystals of **2** and **3** were obtained by slow concentration of methanol solutions containing $Mn(ClO_4)_2 \cdot 6H_2O$, NaN_3, and the appropriate Schiff-base ligands.

IR Spectra

The IR spectra of the three complexes display characteristic bands for the azido bridges and the C=N group. A sharp and strong band at 2067 cm^{-1} in the spectrum of complex **1** is attributed to $\nu_{as}(N_3)$ in the EO mode. For complex **2**, a very strong band at 2067 cm^{-1} with a small shoulder at the higher-frequency side indicates the presence of two different azido groups. Two sharp and strong bands at 2064 and 2095 cm^{-1} indicate the presence of two different azido groups in complex **3**.[3a,7] The characteristic ν(C=N) absorption of the Schiff-base ligands in these complexes appears at around 1595 cm^{-1} as a medium-intensity band.

X-ray Structures

Selected bond lengths and bond angles for the three complexes are summarized in Table 1. The three crystal structures exhibit different hydrogen-bonding patterns, and all the hydrogen-bonding parameters are given in Table 2.

Table 1. Selected bond lengths [Å] and angles [°] for complexes **1**–**3**.

Complex **1**[a]			
Mn(1)–N(1)	2.284(2)	Mn(2)–N(3)	2.294(2)
Mn(1)–N(2)	2.272(2)	Mn(2)–N(4)	2.276(2)
Mn(1)–N(5)	2.225(2)	Mn(2)–N(5)	2.212(2)
Mn(1)–N(8)	2.199(2)	Mn(2)–N(8)	2.192(2)
Mn(1)–N(11)	2.204(2)	Mn(2)–N(14)	2.230(2)
Mn(1)–N(11A)	2.221(2)	Mn(2)–N(14B)	2.198(2)
N(8)–Mn(1)–N(5)	78.06(8)	Mn(1)–N(11)–Mn(1A)	103.96(9)
N(8)–Mn(2)–N(5)	78.49(8)	Mn(2)–N(5)–Mn(1)	100.85(9)
N(11)–Mn(1)–N(11A)	76.04(9)	Mn(2)–N(8)–Mn(1)	102.33(9)
N(14)–Mn(2)–N(14B)	77.5(1)	Mn(2)–N(14)–Mn(2B)	102.5(1)
Complex **2**[b]			
Mn(1)–N(1)	2.299(4)	Mn(1)–N(6)	2.172(3)
Mn(1)–N(2)	2.276(4)	Mn(1)–N(3A)	2.213(3)
Mn(1)–N(3)	2.256(3)	Mn(1)–N(8B)	2.209(4)
N(1)–Mn(1)–N(2)	72.5(1)	N(6)–Mn(1)–N(8B)	90.9(2)
N(3)–Mn(1)–N(3A)	76.5(1)	Mn(1)–N(3)–Mn(1A)	103.5(1)
Complex **3**[c]			
Mn(1)–N(1)	2.287(1)	Mn(1)–N(6)	2.190(1)
Mn(1)–N(2)	2.277(1)	Mn(1)–N(5A)	2.221(2)
Mn(1)–N(3)	2.200(1)	Mn(1)–N(6B)	2.245(1)
N(1)–Mn(1)–N(2)	72.66(5)	N(6)–Mn(1)–N(6B)	78.29(5)
N(3)–Mn(1)–N(5A)	88.75(5)	Mn(1)–N(6)–Mn(1B)	101.71(5)

[a] Symmetry codes: A: $-x, -y, 2-z$; B: $1-x, -y, 2-z$. [b] Symmetry codes: A: $-x, 2-y, 1-z$; B: $0.5+x, 1.5-y, 1-z$. [c] Symmetry codes: A: $1-x, -y, -z$; B: $-x, -y, -z$.

Table 2. Hydrogen-bonding distances [Å] and angles [°] for complexes **1**–**3**.

Complex	D–H···A[a]	D–H	D···A	H···A	∠D–H···A
1	C8–H···N7B	0.93	3.301	2.62	131
	C3–H···N16C	0.93	3.326	2.51	146
	C6–H···N13D	0.93	3.439	2.62	147
	C13–H···N10E	0.93	3.277	2.43	152
2	C7–H···N7A	0.97	3.418	2.47	164
	C6–H···N5C	0.93	3.352	2.56	143
3	C7–H···N3B	0.97	3.477	2.56	157
	C6–H···N8C	0.93	3.392	2.52	157

[a] Symmetry codes for **1**: B: $1-x, -y, 2-z$; C: $-x, -y, 1-z$; D: $x, 0.5-y, -0.5+z$; E: $x, -0.5-y, 0.5+z$. For **2**: A: $-x, 2-y, 1-z$; C: $0.5+x, y, 0.5-z$. For **3**: B: $-x, -y, -z$; C: $x, -1+y, z$.

Complex **1** contains neutral 1D chains constructed by double EO azido bridges linking Mn^{II} ions along the *a* direction. The asymmetric unit consists of a binuclear unit involving two independent Mn^{II} ions, each of which is octahedrally coordinated by six N atoms from a chelating L^1 and four azido ligands in the EO mode [Figure 1(a)]. The binuclear unit is further linked to its two neighbors through two pairs of double EO azido bridges, giving rise to a 1D chain with a Mn(2B)–Mn(2)–Mn(1)–Mn(1A) sequence with three different pairs of bridges between them [Figure 1(b)]. The Mn–N–Mn bridging angles in the centrosymmetric Mn(2B)···Mn(2) and Mn(1)···Mn(1A) pairs are 102.5(1)° and 103.96(9)°, respectively, and those for the noncentrosymmetric Mn(2)···Mn(1) pair are 100.85(9)° and 102.33(9)°. The three different Mn···Mn distances spanned by double EO azido bridges are in the range of 3.420 to 3.486 Å. All the azido ligands are essentially linear, with asymmetric N–N distances. In the lattice, a weak intrachain C–H···N hydrogen bond (Table 2) is formed between the pyridyl group (C8–H) of L^1 and the uncoordinated terminal nitrogen (N7) of the bridging EO azido ligands. Weak interchain C–H···N hydrogen bonds also exist between the azomethine and pyridyl C–H in L^1 and the uncoordinated terminal N atom of the bridging azido ligands [Figure 1(c)]. Neighboring pyridine rings from different chains are parallel to and overlap each other with an interplanar distance of 3.54 Å and a centroid–centroid distance of 4.00 Å; the displacement angle, as defined by Janiak, is about 27.7°.[8] These features indicate a weak π–π stacking interaction between neighboring chains. The nearest interchain Mn···Mn distance is 9.267 Å.

Complex **2** has a 2D layer structure constructed by binuclear units interconnected through single EE azido bridges. A perspective view of the binuclear unit of complex **2** is shown in Figure 2(a). Each Mn^{II} ion is ligated by two N atoms from a chelating L^2 ligand and four azido N atoms, with Mn–N distances ranging from 2.172(3) to 2.299(4) Å. Two neighboring Mn^{II} ions related by an inversion center are linked by double EO azido bridges, the Mn–N–Mn angle and the Mn···Mn distance being 103.5(1)° and 3.509 Å, respectively. Each binuclear unit is linked to four neighboring equivalent units through four single EE azido bridges to form a neutral 2D layer with a pseudo-honeycomb (6,3)

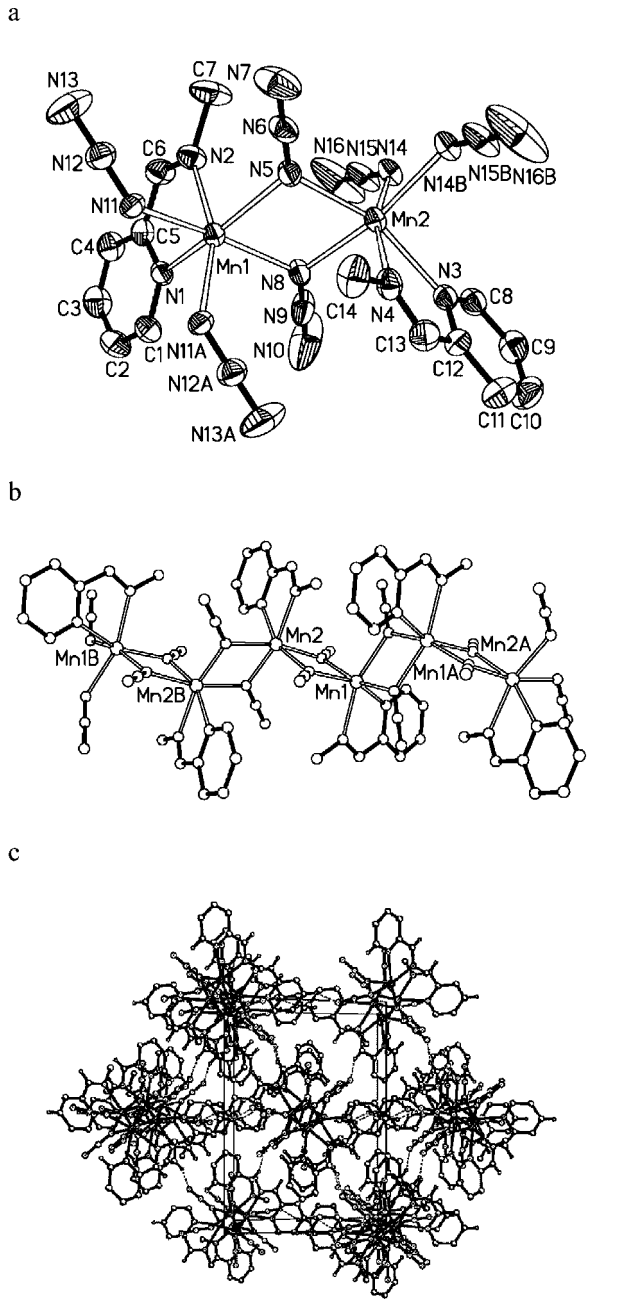

Figure 1. Thermal ellipsoid plot (30% probability), with atom-labeling scheme and H atoms omitted for clarity (a), chain plot (b), and packing of the chains along the *a* direction (c) in **1**.

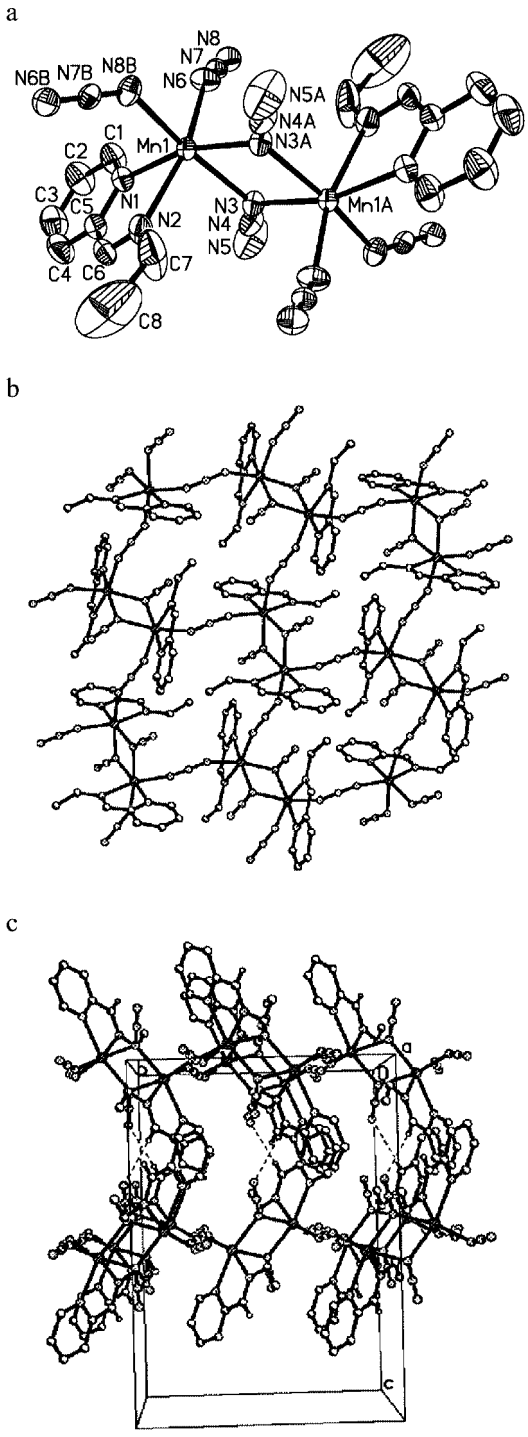

Figure 2. Thermal ellipsoid plot (30% probability), with atom-labeling scheme and H atoms omitted for clarity (a), 2D (6,3) net layer (b), and interactions of neighboring layers (c) in **2**.

topology [Figure 2(b)]. The neighboring Mn_2N_2 units are interrelated by a 2_1 screw operation, with an acute dihedral angle (*a*) between their Mn_2N_2 planar rings (79.5°).

Just like the structures we reported previously,[4i] the structure can also be described as a layer consisting of EE azido-bridged Mn–N_3 helical chains interlinked by double EO azido bridges. The helical chain runs around a twofold screw axis along the *a* direction, and neighboring chains are related by inversion centers and hence have opposite chirality. Within the chain, the Mn–N–N angles are 146.0(3)° and 136.2(3)°, the N–Mn–N angle is 90.9(2)°, and the Mn–N_3–Mn torsion angle (τ) is 7.1°. The Mn···Mn distance spanned by the EE azido bridge is 6.332 Å, and the helical pitch is 10.672 Å.

In the crystal packing, a weak intralayer C–H···N hydrogen bond (Table 2) is formed between the methylene C7–H

of L^2 and the N7 atom of the bridging EE azido ligand. Weak interlayer C–H···N hydrogen bonds also exist between the azomethine C–H of L^2 and the uncoordinated terminal nitrogen of the bridging EO azido ligand from neighboring layers [Figure 2(c)]. The 2D layers are stacked down the *c* direction, with the minimum interlayer Mn···Mn distance being 9.257 Å, which is significantly shorter than the distances found in most 2D Mn–azido systems. This short interlayer separation in **2** may be a consequence of deep complementary interdigitation between the consecutive layers. As can be seen from Figure 2(c), the pyridine groups of the L^2 ligands on each side of a layer extend deeply into the "empty" space of neighboring layers.

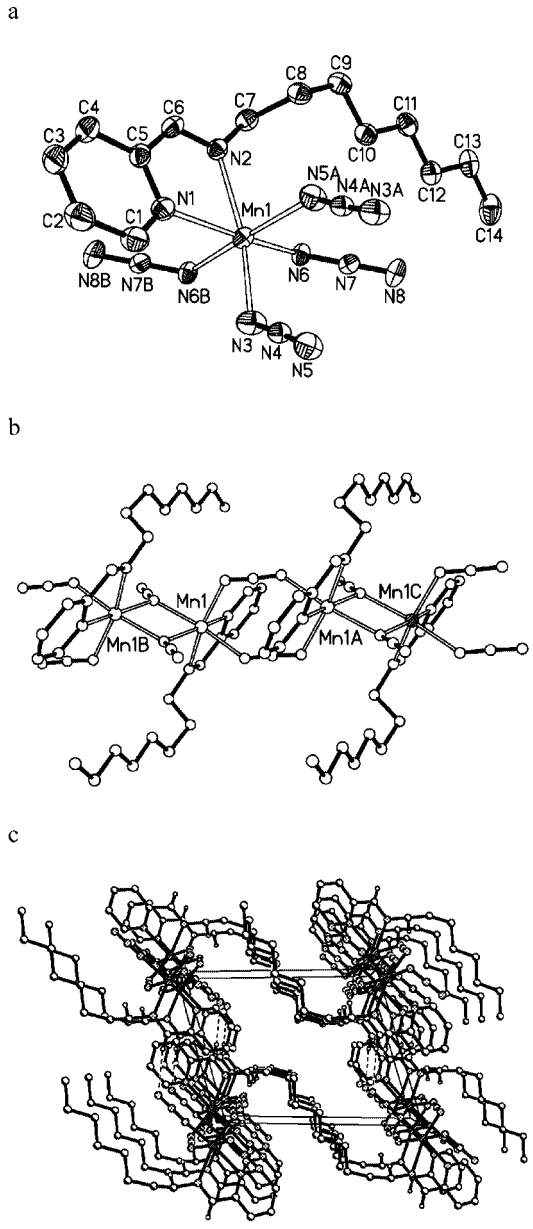

Figure 3. Thermal ellipsoid plot (30% probability), with atom-labeling scheme and H atoms omitted for clarity (a), chain plot (b) and packing of the chains along the *a* direction (c) in **3**.

In complex **3**, each Mn^{II} center exhibits a distorted octahedral MnN_6 coordination sphere and is bonded by two EO and two EE azides with two N atoms from the chelate Schiff-base L^3 (Figure 3). Neighboring Mn^{II} ions are linked alternately by double EO and double EE azido bridges to form an alternate chain running along the *a* direction. All the Mn–N distances are in the range of 2.190(1) to 2.287(1) Å. The small chelate angle [N1–Mn1–N2 = 72.66(5)°] indicates the severe distortion of the Mn^{II} coordination geometry. The EO azido bridges possess asymmetric N–N distances, while the EE bridges are essentially symmetric. In the EO bridging moiety, the Mn1–N6–Mn1B angle and the Mn···Mn distance are 101.71(5)° and 3.440 Å, respectively. In the EE bridging moiety, the Mn–N–N angles are 126.1(1)° and 141.3(1)° and the Mn–N_3–Mn torsion angle is 15.9°. The dihedral angle between the (EE–N_3)$_2$ plane and the N5–Mn1–N3A plane is only 7.6°, thereby indicating a slight chair conformation for the Mn–(N$_3$)$_2$–Mn ring. The Mn···Mn distance separated by EE bridges is 5.466 Å.

In the crystal packing, a weak intrachain C–H···N hydrogen bond (Table 2) exists between the methylene C7–H of L^3 and the coordinated nitrogen (N3) of the bridging EE azido ligand. The azomethine C–H group of the L^3 also forms a weak interchain C–H···N hydrogen bond with the uncoordinated terminal N atom of the bridging EO azido ligands from neighboring chains along the *b* direction [Figure 3(c)]. The long tails of the L^3 ligands from neighboring chains interdigitate one another and separate the chains by 12.007 Å. Neighboring pyridine rings from different chains parallel and overlap each other with an interplanar distance of 3.52 Å and a centroid–centroid distance of 3.80 Å; the displacement angle is about 22.0°.[8] These features indicate weak π–π stacking interactions between neighboring chains. The minimum interchain Mn···Mn distance is 8.556 Å along the *b* direction.

Magnetic Properties

Complex 1

The magnetic susceptibility of **1** was measured at a field of 5 kOe in the temperature range 2–300 K [Figure 4(a)]. The temperature dependence of χ_M^{-1} above 21 K obeys the Curie–Weiss law with a positive Weiss constant (θ = 15.91 K), indicating an intrachain ferromagnetic interaction, as expected for the azido bridges in the double EO mode. The room-temperature $\chi_M T$ value is around 4.41 emu K mol^{-1} per Mn^{II} ion, which is close to the spin-only value (4.38 emu K mol^{-1}) for a high-spin Mn^{II} ion. Upon cooling, $\chi_M T$ increases smoothly to a maximum at about 6 K, and then decreases rapidly. This may indicate an overall intrachain ferromagnetic interaction and an interchain antiferromagnetic interaction. The magnetic behavior of **1** was analyzed by fitting the experimental susceptibility to Fisher's calculation[9] for a classical or infinite spin chain, scaled to a real spin of 5/2.[10] The expression for

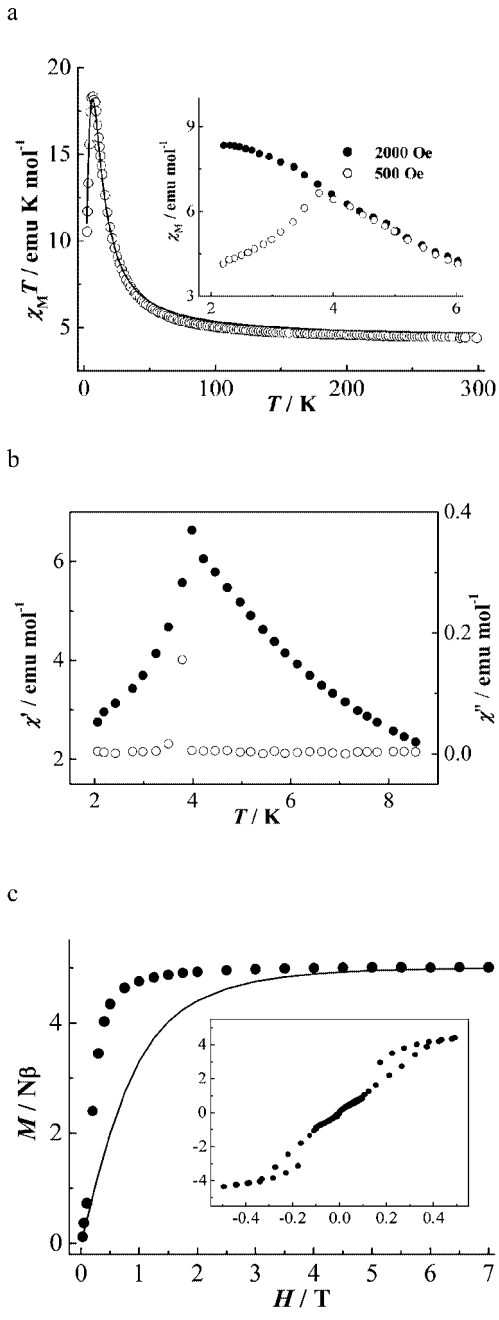

Figure 4. (a) $\chi_M T$ vs. T plot of **1**. The solid line was plotted according to the fit parameters given in the text. Inset: fc magnetization curves at 500 and 2000 Oe. (b) Temperature-dependence of the ac magnetic susceptibility at zero applied dc field and an ac field of 2 Oe and 277 Hz. (c) Field dependence of the magnetization. The solid line was plotted according to the Brillouin function for an S = 5/2 system with g = 2. The inset is the hysteresis loop at 1.8 K.

the magnetic susceptibility is given by Equation (1), where $u = (T/T_o) - \coth(T_o/T)$ with $T_o = JS(S + 1)/k$.

$$\chi_{chain} = [Ng^2\beta^2S(S + 1)/(3kT)][(1 - u)/(1 + u)] \quad (1)$$

The J parameter is based on the spin-Hamiltonian $H = -J\Sigma S_iS_{i+1}$. The interchain interaction (zJ') was accounted for by the molecular-field approximation [Equation (2)].[14]

$$\chi_M = \chi_{chain}/[1 - (zJ'/Ng^2\beta^2)\chi_{chain}] \quad (2)$$

The best fit leads to J = 2.54(2) cm^{-1} and zJ' = –0.41(5) cm^{-1}, with the g-value fixed at 2.0.

Although double EO azido bridges have been found in many metal azide complexes, chains with exclusive double EO azido bridges are still rare. One such compound, [Mn(2-bzpy)$(N_3)_2]_n$ (2-bzpy = 2-benzoylpyridine), which also exhibits ferromagnetic intrachain interactions, has been reported previously.[3d] Compared with EO azido-bridged complexes with similar structures, it has been suggested that the M–N–M bridging angle (θ) is the main factor that controls the magnetic interaction between metal ions. The ferromagnetic intrachain interaction (J = 2.54 cm^{-1}) for **1**, in which the bridging angles average to 102.4°, is stronger than that (J = 0.8 cm^{-1}) for [Mn(2-bzpy)$(N_3)_2]_n$, in which the average bridging angle (100.5°) is smaller. This trend is consistent with the density functional calculations on model Mn^{II} compounds performed by Ruiz et al.[12] This calculation predicts that a crossover between ferro- and antiferromagnetic interactions occurs at θ = 98°, and that the ferromagnetic interaction increases when the Mn–N–Mn bridging angle increases above 98°.[12]

To investigate further the magnetic behavior of **1**, field-cooled (fc) magnetization at different fields was measured and the plot is given in Figure 4(a, inset). At 500 Oe, the magnetization presents a maximum at around 3.7 K, suggesting the onset of 3D antiferromagnetic ordering among the ferromagnetic chains. However, the magnetization at 2 kOe shows no maximum and tends to saturate at lower temperature, thus indicating that the interchain antiferromagnetic interaction is overcome by the external field. These features are indicative of a metamagnet built of ferromagnetic chains. The temperature dependence of the ac magnetic susceptibility was also measured at zero dc field and confirmed the occurrence of the magnetic ordering, with T_N = 3.9 K, at which both χ' (the in-phase component) and χ'' (the out-of-phase component) reach maximum values [Figure 4(b)].

The metamagnetic behavior was confirmed by the field dependence of the magnetization, as shown in Figure 4(c). The sigmoid shape of the M vs. H curve at 1.8 K clearly indicates a field-induced transition from an antiferromagnetic to a ferromagnetic state, which is characteristic of a metamagnet. The critical field is about 2 kOe, estimated as the field at which a maximum $\partial M/\partial H$ value is reached. Upon increasing the field, the magnetization increases rapidly and saturates at 5.0 $N\beta$, and the saturation is much more rapid than that predicted by the Brillouin function. This definitely confirms the presence of ferromagnetic interactions. Hysteresis loop measurements revealed that **1** is a metamagnet with a typical crossover magnetic hysteresis [Figure 4(c, inset)].

In contrast to **1**, the previous compound [Mn(2-bzpy)$(N_3)_2]_n$ does not exhibit long-range magnetic ordering above 2 K. This may be due to its longer interchain Mn···Mn distance of 9.931 Å than that of **1** (9.267 Å), which weakens the interchain interactions.

Complex 2

The magnetic susceptibility of **2** was measured in the range 2–300 K at 5 kOe and is shown as χ_M vs. T and $\chi_M T$ vs. T plots in Figure 5(a). The $\chi_M T$ value at 300 K is about 3.91 emu K mol^{-1}. Upon cooling, $\chi_M T$ decreases monotonically and vanishes when T approaches zero, indicating an overall antiferromagnetic interaction. As the temperature is lowered, χ_M value increases first to a rounded maximum of 0.045 emu mol^{-1} at about 36 K, then decreases to a minimum value of 0.044 emu mol^{-1} at 21 K, and finally increases to 0.045 emu mol^{-1} at 2 K. The behaviors above 20 K are typical of 1D and 2D Mn^{II} complexes with dominant antiferromagnetic interactions, and the increase of χ_M below 20 K may be due to the presence of a spin-canted structure (see below).

To evaluate the magnetic interactions via the azido bridges in **2**, we used an approximate approach that has been used for similar compounds.[4e,4i] This approach treats the 2D layer as EE azido-bridged antiferromagnetic chains interacting ferromagnetically through the double EO azido bridges. Consequently, Equations (1) and (2) are applicable, where J is the interaction through the EE azido bridge and zJ' is the interaction through the double EO azido bridges. The least-squares fit of the experimental data above 26 K to the above expressions led to J = –4.85(4) cm^{-1} and zJ' = 2.5(4) cm^{-1} with g = 2.0. These values are comparable to those for related compounds and confirm that the interactions mediated by the single EE and the double EO bridges are antiferro- and ferromagnetic, respectively. Selected structural and magnetic parameters for **2** and similar 2D Mn^{II}–azido complexes are collected in Table 3 for comparison. EHMO calculations have shown that the antiferromagnetic interactions through the single EE azido bridge should maximize as the Mn–N–N bond angle approaches 110° and the Mn–N_3–Mn torsion angle (τ) approaches 0 or 180°.[4b] The data listed in Table 3 suggest that the influence of the torsion angle dominates in these systems: the strongest interaction is observed for compound **I**, in which the torsion angle is 180°, although the compound has the largest Mn–N–N angles. On the other hand, compound **III**, which has a torsion angle close to 90°, exhibits the lowest |J| value, although the Mn–N–N angles are the closest to 110°. Other compounds, including **2**, have in-between angles (the torsion angles are between 90 and 180 or 0°) and J values. The interaction parameters of the double azido bridges for these complexes fall in the range 1.1–3.1 cm^{-1}, with the Mn–N–Mn angles in the narrow range of 100.8–103.5°. Apparently, the general trend whereby the ferromagnetic interaction increases with increasing bridging angle is not well followed: the largest J value is obtained for the compound that has a relatively small angle (compound **II**, 101.9°), and the compound that has the largest angle exhibits a relatively small J value (compound **2**, 2.5 cm^{-1}). This may be due to the

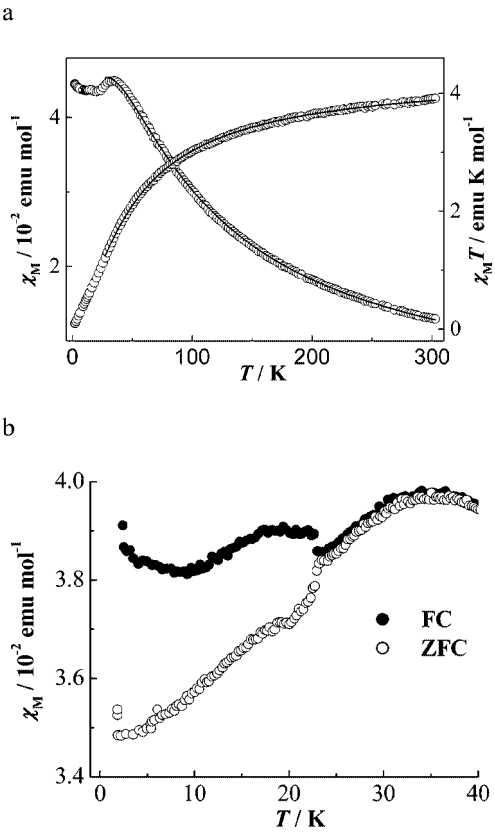

Figure 5. (a) χ_M and $\chi_M T$ vs. T plots for **2**. The solid line was plotted according to the fit parameters given in the text. (b) zfc and fc magnetization at 200 Oe.

Table 3. Structural and magnetic parameters for double EO and single EE 2D Mn^{II}–azido complexes containing a (6,3) network.

Complex[a]	$[Mn(dmbpy)(N_3)_2]_n$, **I**	$[Mn(2\text{-}bphz)(N_3)_2]_n$, **II**	$[Mn(mpci)(N_3)_2]_n$, **III**	$[Mn(4\text{-}Etpy)(N_3)_2]_n$, **IV**	$[Mn(L^2)(N_3)_2]_n$, **2**
J_{EE} [cm^{-1}]	–5.4	–5.1	–4.6	–5.3	–4.85
M–N–N [°][b]	163.8, 153.9	158.1, 150.9	131.7, 132.3	150.3, 143.9	136.2(3), 146.0(3)
τ [°][c]	180	21.5	92.4	17.6	7.1
M···M(EE) [Å]	6.611, 6.537	6.496	5.810	6.083	6.332
J_{EO} [cm^{-1}]	1.7	3.1	1.1	2.9	2.5
M–N–M [°][d]	102.2	101.9	100.8	102.2	103.5(1)
M···M(EO) [Å]	3.533	3.459	3.426	3.523	3.509
α [°][e]	0	78.9	83.7	86.7	79.5
Canting	no	yes	yes	yes	yes
Ref.	[4e]	[4i]	[4i]	[4g]	this work

[a] Dmbpy = 4,4′-dimethyl-2,2′-bipyridine; 2-bphz = 2-benzoylpyridine hydrazone; mpci = methyl pyrazinecarboximidate; 4-Etpy = 4-ethylpyridine; L^2 = *N*-(2-pyridylmethylene)ethylamine. [b] For the EE azido bridging moiety. [c] The M–N–N–N–M torsion angle. [d] For the EO azido bridging moiety. [e] The dihedral angle between the neighboring planar Mn_2N_2 rings.

operation of other factors such as Mn–N bond lengths and coordination environments, which should influence the magnetic orbitals around the metal center.

It has been shown that, except for compound **I** in Table 3, all the previous layered compounds with double EO and single EE bridges exhibit spin-canting behavior, which is consistent with the structural observation that the coordination polyhedra (or the double EO bridged Mn_2N_2 moieties) linked by the single EE azido bridges are slanted with respect to each other.[4b,4d,4g,4i] The absence of spin-canting in **I** has been related to the crystallographic centrosymmetry of the single EE azido bridges.[4e,4i] According to the structural data, **2** should exhibit a spin-canted structure. To confirm this point, the field-cooled and zero-field-cooled (zfc) magnetizations were measured at an applied field of 200 Oe [Figure 5(b)]. It is evident that the complex exhibits weak spontaneous magnetization below 22 K, which is characteristic of weak ferromagnets due to the spin-canting. Field-dependent magnetizations at 2 K were also measured, and the magnetization at 50 kOe is 0.46 $N\beta$, far below the saturation value expected for an $S = 5/2$ system (5.0 $N\beta$ with $g = 2.0$). No hysteresis was detected.

Complex 3

The magnetic susceptibility of **3** was measured in the temperature range 2–300 K at 20 kOe. The χ_M and $\chi_M T$ vs. T plots are shown in Figure 6. The experimental $\chi_M T$ value at 300 K is 3.63 emu K mol^{-1}. Upon cooling, the $\chi_M T$ product decreases monotonically, indicating a dominant antiferromagnetic interaction. The χ_M value increases monotonically, and a rapid increase below 17 K may be caused by the presence of a small amount of paramagnetic impurities.

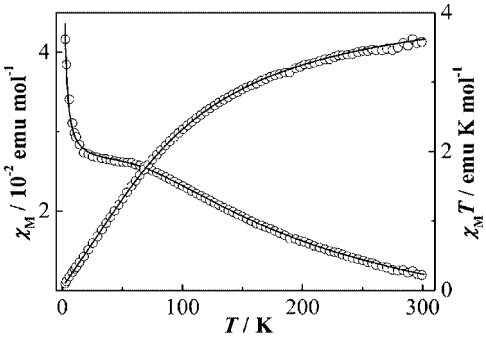

Figure 6. χ_M and $\chi_M T$ vs. T plots of **3**. The solid line was plotted according to the fit parameters given in the text.

According to the structural data, complex **3** should possess alternating ferro- and antiferromagnetic interactions mediated by double EO and double EE azido bridges, respectively.[3a,3d,3i] To simulate the experimental magnetic behavior, we used a theoretical model proposed by Cortés et al. for alternating $S = 5/2$ chains.[3a] The nearest-neighbor exchange interactions are described by the spin-Hamiltonian given in Equation (3). The expression of the molar susceptibility is given by Equation (4).

$$H = -J_1\Sigma S_{2i}S_{2i+1} - J_2\Sigma S_{2i+1}S_{2i+2} \quad (3)$$

$$\chi_M = [Ng^2\beta^2S(S+1)/3kT]\{[(1+u_1+u_2+u_1u_2)/(1-u_1u_2)](1-\rho)+\rho\} \quad (4)$$

where $u_i = \coth[J_iS(S+1)/kT] - kT/[J_iS(S+1)]$ ($i = 1, 2$). In this expression we have included a ρ parameter, which is related to the amount of paramagnetic impurities (presumably a monomeric Mn^{II} complex), to account for the in-

Table 4. Structural and magnetic parameters for alternating double EE and double EO 1D Mn^{II}–azido complexes.

Complex[a]	Mn–N–Mn [°]	J_F [cm^{-1}]	δ [°]	J_{AF} [cm^{-1}]	Ref.
$[Mn(bipy)(N_3)_2]_n$	101.0	9.6	22.7	–11.9	[3a]
$[Mn(3\text{-}bzpy)_2(N_3)_2]_n$	100.4	3.5	26.6	–12.3	[3d]
$[Mn(3\text{-}Et,4\text{-}Mepy)_2(N_3)_2]_n$	99.7	2.4	31.7	–13.7	[3c]
$[Mn(bpm)(N_3)_2]_n$	102.9	**1.8**	20.5	**–7.3**	[3e]
		(15.7)[b]		(–63.7)[b]	[3e]
$[Mn(dpa)(N_3)_2]_n$	102.9	**5.2**	35.1	**–6.1**	[3h]
		(45.3)[b]		(–53.3)[b]	[3h]
$[Mn(L1)(N_3)_2]_n$	99.6	3.8	9.8	–15.4	[3i]
$[Mn(L2)(N_3)_2]_n$	101.6	5.2	–	–11.8	[3i]
	101.1				[3i]
$[Mn(L3)(N_3)_2]_n$	103.9	7.2	19.5	–13.7	[3i]
$[Mn(L4)(N_3)_2]_n$	100.6	4.1	9.8	–13.3	[3i]
$[Mn(L5)(N_3)_2]_n$	104.0	8.0	12.0	–14.4	[3i]
$[Mn(L)(N_3)_2]_n$	102.0	5.6	19.6	–11.9	[3j]
$[Mn(TaiEt)(N_3)_2]_n$	103.5	2.7	1.8	–14.5	[3k]
$\{[Mn(N_3)_2(3\text{-}Clpy)_2](3\text{-}Clpy)_{0.5}\}_n$	100.5	6.0	9.8	–16.7	[3n]
$[\{Mn(N_3)_2\}_2L']_n$	77.2	3.8	2.9	–8.1	[6e]
$[Mn(L^3)(N_3)_2]_n$ (**3**)	101.7	1.6	7.6	–13.9	this work

[a] Bipy = 2,2′-bipyridine; 3-bzpy = 3-benzoylpyridine; 3-Et,4-Mepy = 3-ethyl-4-methylpyridine; bpm = bis(pyrazol-1-yl)methane; dpa = 2,2′-dipyridylamine; L1 = *N*-phenyl-2-carbaldimine; L2 = *N*-(*p*-tolyl)-2-carbaldimine; L3 = *N*-(*m*-tolyl)-2-carbaldimine; L4 = *N*-(*p*-chlorophenyl)-2-carbaldimine; L5 = *N*-(*m*-chlorophenyl)-2-carbaldimine; L = 2-(pyrazol-1-ylmethyl)pyridine; TaiEt = 1-ethyl-2-(*p*-tolylazo)imidazole; 3-Clpy = 3-chloropyridine; L′ = 4,5-diazafluoren-9-one azine; L^3 = *N*-(2-pyridylmethylene)octylamine. [b] The recalculated values are indicated in bold and the values in parentheses are those reported in the references. After checking the data carefully, we believe that the J values reported in refs.[3e,3h] are actually for $JS(S+1)$.

crease of χ_M below 17 K. The best fit of the experimental data led to J_1 = 1.6(2) cm^{-1}, J_2 = –13.9(1) cm^{-1}, and ρ = 0.01 with g fixed at 2.0. The J_1 and J_2 parameters verify the alternating ferro- and antiferromagnetic interactions, with the antiferromagnetic one dominating.

A chain structure with alternating double EO and double EE azido bridges is the most frequently encountered Mn–azido motif. In our previous work,[3i] this class of Mn^{II} compounds follows the general trend that the ferromagnetic interaction through the double EO bridge increases with the Mn–N–Mn angle, and that the antiferromagnetic interaction through the double EE bridge decreases with the increase of the dihedral angle (δ) between the $(N_3)_2$ plane and the N(EE azido)–Mn–N(EE azido) plane. Since then, several new compounds have been characterized structurally and magnetically. Relevant structural and magnetic data for the known compounds, along with **3**, are collected in Table 4 for comparison. As can be seen, the general trends, which have also been demonstrated by theoretical studies,[3a,12] are followed by most compounds, but it should be noted that there are some evident deviations. The most remarkable example is $[\{Mn(N_3)_2\}_2L']_n$, in which Mn^{II} chains with alternating double EO and double EE azido bridges are linked into a 3D network by 4,5-diazafluoren-9-one azine (L′):[6e] the double EO bridge with a much smaller Mn–N–Mn angle (77°) than the AF–F crossover angle (98°) predicted by density functionl calculations mediates a ferromagnetic interaction, instead of antiferromagnetic interaction, and the double EE bridge with a very small δ angle (2.9°) mediates a relatively weak antiferromagnetic interaction. For **3** and $[Mn(TaiEt)(N_3)_2]_n$,[3k] the J_{EO} values seem to be too small for their medium and large M–N–M angles, respectively. These deviations may be due to the influence of other structural parameters. Further pragmatic but laborious studies are therefore needed to get more accurate magneto-structural correlations.

Conclusions

We have presented the syntheses, structures, and magnetic properties of three new azido-bridged Mn^{II} coordination polymers with flexible tail co-ligands. With increasing steric demand of the co-ligands L^1, L^2, and L^3, the structures vary from a double EO azido-bridged uniform chain (**1**), through a double EO and single EE azido-bridged 2D layer (**2**), to a double EO and double EE azido-bridged alternate chain (**3**), respectively. Magnetically, **1** is a metamagnet built of ferromagnetic chains, **2** exhibits a weak ferromagnetism due to spin-canting, and **3** shows alternate ferro- and antiferromagnetic intrachain interactions. We are currently working with other flexible tail co-ligands by varying their substituents to get more information about the relationship between the final structures and the co-ligands and to study their magnetic behaviors towards the preparation of molecule-based magnetic materials.

Experimental Section

Materials and Physical Measurements: All the starting chemicals were of A.R. grade and were used as received. The Schiff-base ligands L^1, L^2, and L^3 were prepared according to literature procedures.[13] Elemental analyses (C,H,N) were performed on an Elementar Vario EL analyzer. IR spectra were recorded with a Nicolet Magna-IR 750 spectrometer equipped with a Nic-Plan Microscope. Temperature- and field-dependent magnetic measurements were carried out on an Oxford MagLab 2000 magnetometer. Diamagnetic corrections were made with Pascal's constants.[14]

Caution! *Azide and perchlorate complexes of metal ions are potentially explosive. Only a small amount of the materials should be prepared, and it should be handled with care.*

$[Mn(L^1)(N_3)_2]_n$ (1): A methanol solution (10 mL) containing $Mn(ClO_4)_2{\cdot}6H_2O$ (0.181 g, 0.5 mmol) and L^1 (0.061 g, 0.5 mmol), and a methanol solution (10 mL) of NaN_3 (0.065 g, 1.0 mmol) were added respectively to the two arms of an H-tube, then methanol was carefully added to both arms until the bridge of the tube was filled. Slow interdiffusion of the two solutions afforded yellow crystals of **1** after two weeks. Yield: 0.042 g (32%). $C_{14}H_{16}Mn_2N_{16}$ (518.31): calcd. C 32.45, H 3.11, N 43.24; found C 32.48, H 3.30, N 43.50. IR: $\tilde{\nu}$ = 2067 vs, 1595 m, 1441 m, 1334 m, 1305 m, 1283 m, 1014 m, 775 m cm^{-1}.

$[Mn(L^2)(N_3)_2]_n$ (2): A methanol solution (10 mL) of $Mn(ClO_4)_2{\cdot}6H_2O$ (0.181 g, 0.5 mmol) was added to a solution of L^2 (0.068 g, 0.5 mmol) in the same solvent. The mixture was stirred for 5 min, then a methanol (10 mL) solution of NaN_3 (0.065 g, 1 mmol) was added with continuous stirring. Slow evaporation of the resulting orange solution at room temperature yielded yellow crystals after two weeks. Yield: 0.080 g (59%). $C_8H_{10}MnN_8$ (273.18): calcd. C 35.18, H 3.69, N 41.02; found C 35.14, H 3.85, N 41.42. IR: $\tilde{\nu}$ = 2067 s, 1595 m, 1479 m, 1475 m, 1443 m, 1339 m, 1305 m, 1156 m, 1106 m, 1013 m, 779 m cm^{-1}.

$[Mn(L^3)(N_3)_2]_n$ (3): This complex was prepared in the same way as **2**, using L^3 instead of L^2. Yield: 0.043 g (24%). $C_{14}H_{22}MnN_8$ (357.34): calcd. C 47.06, H 6.21, N 31.36; found C 47.07, H 6.27, N 31.79. IR: $\tilde{\nu}$ = 2095 vs, 2064 vs, 1595 m, 1467 m, 1442 m, 1334 m, 1013 m, 775 m cm^{-1}.

X-ray Crystallographic Study: Diffraction intensity data for single crystals of **1**, **2**, and **3** were collected at room temperature on a Nonius Kappa CCD area detector equipped with graphite-mono-

Table 5. Summary of crystallographic data for complexes **1**–**3**.

	1	**2**	**3**
Empirical formula	$C_{14}H_{16}Mn_2N_{16}$	$C_8H_{10}MnN_8$	$C_{14}H_{22}MnN_8$
Formula mass	518.31	273.18	357.34
Crystal system	monoclinic	orthorhombic	triclinic
Space group	$P2_1/c$	$Pbca$	$P\bar{1}$
a [Å]	12.016(2)	10.6725(2)	8.1436(2)
b [Å]	16.589(3)	12.6390(3)	9.4498(2)
c [Å]	11.867(2)	17.6030(5)	12.3898(4)
α [°]	90	90	72.8132(9)
β [°]	103.51(3)	90	76.3392(9)
γ [°]	90	90	82.161(1)
V [Å^3]	2300.0(8)	2374.5(1)	882.84(4)
Z	4	8	2
$D_{calcd.}$ [g cm^{-3}]	1.497	1.528	1.344
μ [mm^{-1}]	1.135	1.103	0.759
R_1 [$I > 2\sigma(I)$]	0.0352	0.0529	0.0328
wR_2 (all data)	0.0822	0.1663	0.0795
GOF	0.880	0.947	0.990

chromated Mo-K_α radiation (λ = 0.71073 Å). Empirical absorption corrections were applied using the Sortav program.[15] The structures were solved by direct methods and refined by full-matrix least-squares on F^2 with anisotropic thermal parameters for all non-hydrogen atoms.[11] Hydrogen atoms were placed geometrically and refined isotropically. Pertinent crystallographic data and structure refinement parameters are summarized in Table 5.

CCDC-279815 (for **1**), -279816 (for **2**), and -279817 (for **3**) contain the supplementary crystallographic data for this paper. These data can be obtained free of charge from The Cambridge Crystallographic Data Center via www.ccdc.cam.ac.uk/data_request/cif.

Acknowledgments

We acknowledge the NSFC (grant nos. 20221101, 20201009, and 20490210) and the Foundation of Science and Technology Development of Shanghai (03ZR14024) for financial support.

[1] a) O. Kahn, *Molecular Magnetism*, Wiley, New York, **1993**; b) *Molecular Magnets: Recent Highlights* (Eds.: W. Linert, M. Verdaguer), Springer, Wien, New York, **2003**.

[2] a) *Magnetism: Molecules to Materials* (Eds.: J. S. Miller, M. Drillon), Wiley VCH, Weinheim (Germany), **2001**; b) J. Ribas, A. Escuer, M. Monfort, R. Vicente, R. Cortés, L. Lezama, T. Rojo, *Coord. Chem. Rev.* **1999**, *193–195*, 1027–1068.

[3] a) R. Cortés, M. Drillon, X. Solans, L. Lezama, T. Rojo, *Inorg. Chem.* **1997**, *36*, 677–683; b) A. Escuer, R. Vicente, M. A. S. Goher, F. A. Mautner, *Inorg. Chem.* **1998**, *37*, 782–787; c) M. A. M. Abu-Youssef, A. Escuer, M. A. S. Goher, F. A. Mautner, R. Vicente, *Eur. J. Inorg. Chem.* **1999**, 687–691; d) M. A. M. Abu-Youssef, A. Escuer, D. Gatteschi, M. A. S. Goher, F. A. Mautner, R. Vicente, *Inorg. Chem.* **1999**, *38*, 5716–5723; e) L.-F. Tang, L. Zhang, L.-C. Li, P. Cheng, Z.-H. Wang, J.-T. Wang, *Inorg. Chem.* **1999**, *38*, 6326–6328; f) M. A. M. Abu-Youssef, A. Escuer, M. A. S. Goher, F. A. Mautner, G. J. Reiβ, R. Vicente, *Angew. Chem. Int. Ed.* **2000**, *39*, 1624–1626; g) M. A. M. Abu-Youssef, M. Drillon, A. Escuer, M. A. S. Goher, F. A. Mautner, R. Vicente, *Inorg. Chem.* **2000**, *39*, 5022–5027; h) M. Villanueva, J. L. Mesa, M. K. Urtiaga, R. Cortés, L. Lezama, M. I. Arriortua, T. Rojo, *Eur. J. Inorg. Chem.* **2001**, 1581–1586; i) E.-Q. Gao, S.-Q. Bai, Y.-F. Yue, Z.-M. Wang, C.-H. Yan, *Inorg. Chem.* **2003**, *42*, 3642–3649; j) E.-Q. Gao, S.-Q. Bai, C.-F. Wang, Y.-F. Yue, C.-H. Yan, *Inorg. Chem.* **2003**, *42*, 8456–8464; k) U. Ray, S. Jasimuddin, B. K. Ghosh, M. Monfort, J. Ribas, G. Mostafa, T.-H. Lu, C. Sinha, *Eur. J. Inorg. Chem.* **2004**, 250–259; l) J. Cano, Y. Journaux, M. A. S. Goher, M. A. M. Abu-Youssef, F. A. Mautner, G. J. Reiβ, A. Escuer, R. Vicente, *New J. Chem.* **2005**, *29*, 306–314; m) S. Deoghoria, S. K. Bera, B. Moulton, M. J. Zaworotko, J.-P. Tuchagues, G. Mostafa, T.-H. Lu, S. K. Chandra, *Polyhedron* **2005**, *24* 343–350; n) M. A. M. Abu-Youssef, A. Escuer, R. Vicente, F. A. Mautner, L. Öhrstrom, M. A. S. Goher, *Polyhedron* **2005**, *24*, 557–562.

[4] a) A. Escuer, R. Vicente, M. A. S. Goher, F. A. Mautner, *Inorg. Chem.* **1995**, *34*, 5707–5708; b) A. Escuer, R. Vicente, M. A. S. Goher, F. A. Mautner, *Inorg. Chem.* **1996**, *35*, 6386–6391; c) A. Escuer, R. Vicente, M. A. S. Goher, F. A. Mautner, *J. Chem. Soc., Dalton Trans.* **1997**, 4431–4434; d) A. Escuer, R. Vicente, M. A. S. Goher, F. A. Mautner, *Inorg. Chem.* **1997**, *36*, 3440–3446; e) Z. Shen, J.-L. Zuo, Z. Yu, Y. Zhang, J.-F. Bai, C.-M. Che, H.-K. Fun, J. J. Vittal, X.-Z. You, *J. Chem. Soc., Dalton Trans.* **1999**, 3393–3398; f) M. A. S. Goher, M. A. M. Abu-Youssef, F. A. Mautner, R. Vicente, A. Escuer, *Eur. J. Inorg. Chem.* **2000**, 1819–1823; g) A. Escuer, J. Cano, M. A. S. Goher, Y. Journaux, F. Lloret, F. A. Mautner, R. Vicente, *Inorg. Chem.* **2000**, *39*, 4688–4695; h) E.-Q. Gao, S.-Q. Bai, Z.-M. Wang, C.-H. Yan, *J. Am. Chem. Soc.* **2003**, *125*, 4984–4985; i) E.-Q. Gao, Y.-F. Yue, S.-Q. Bai, Z. He, S.-W. Zhang, C.-H. Yan, *Chem. Mater.* **2004**, *16*, 1590–1596; j) E.-Q. Gao, Y.-F. Yue, S.-Q. Bai, Z. He, C.-H. Yan, *J. Am. Chem. Soc.* **2004**, *126*, 1419–1429; k) A. Escuer, F. A. Mautner, M. A. S. Goher, M. A. M. Abu-Youssef, R. Vicente, *Chem. Commun.* **2005**, 605–607.

[5] a) F. A. Mautner, R. Cortés, L. Lezama, T. Rojo, *Angew. Chem. Int. Ed. Engl.* **1996**, *35*, 78–80; b) F. A. Mautner, S. Hanna, R. Cortés, L. Lezama, M. G. Barandika, T. Rojo, *Inorg. Chem.* **1999**, *38*, 4647–4652; c) M. A. S. Goher, J. Cano, Y. Journaux, M. A. M. Abu-Youssef, F. A. Mautner, A. Escuer, R. Vicente, *Chem. Eur. J.* **2000**, *6*, 778–784.

[6] a) G. De Munno, M. Julve, G. Viau, F. Lloret, J. Faus, D. Viterbo, *Angew. Chem. Int. Ed. Engl.* **1996**, *35*, 1807–1810; b) R. Cortés, L. Lezama, J. L. Pizarro, M. I. Arriortua, T. Rojo, *Angew. Chem. Int. Ed. Engl.* **1996**, *35*, 1810–1812; c) H.-Y. Shen, D.-Z. Liao, Z.-H. Jiang, S.-P. Yan, B.-W. Sun, G.-L. Wang, X.-K. Yao, H.-G. Wang, *Chem. Lett.* **1998**, 469–470; d) S. Martín, M. G. Barandika, L. Lezama, J. L. Pizarro, Z. E. Serna, J. I. Ruiz de Larramendi, M. I. Arriortua, T. Rojo, R. Cortés, *Inorg. Chem.* **2001**, *40*, 4109–4115; e) C.-M. Liu, S. Gao, D.-Q. Zhang, Y.-H. Huang, R.-G. Xiong, Z.-L. Liu, F.-C. Jiang, D.-B. Zhu, *Angew. Chem. Int. Ed.* **2004**, *43*, 990–994; f) E.-Q. Gao, Z.-M. Wang, C.-H. Yan, *Chem. Commun.* **2003**, 1748–1749; g) H.-L. Sun, S. Gao, B.-Q. Ma, G. Su, S. R. Batten, *Cryst. Growth Des.* **2005**, *5*, 269–277; h) A. K. Ghosh, D. Ghoshal, E. Zangrando, J. Ribas, N. Ray Chaudhuri, *Inorg. Chem.* **2005**, *44*, 1786–1793.

[7] S. S. Tandon, L. K. Thompson, M. E. Manuel, J. N. Bridson, *Inorg. Chem.* **1994**, *33*, 5555–5570.

[8] C. Janiak, *J. Chem. Soc., Dalton Trans.* **2000**, 3885–3896.

[9] M. E. Fisher, *Am. J. Phys.* **1964**, *32*, 343–346.

[10] R. Dingle, M. E. Lines, S. L. Holt, *Phys. Rev.* **1969**, *187*, 643–648.

[11] a) G. M. Sheldrick, *SHELXTL* Version 5.1. Bruker Analytical X-ray Instruments Inc., Madison, Wisconsin, USA, **1998**; b) G. M. Sheldrick, *SHELXL-97*, PC Version, University of Göttingen, Germany, **1997**.

[12] E. Ruiz, J. Cano, S. Alvarez, P. Alemany, *J. Am. Chem. Soc.* **1998**, *120*, 11122–11129.

[13] P. Bamfield, R. Price, R. G. J. Miller, *J. Chem. Soc., A* **1969**, 1447–1452.

[14] C. J. O'Connor, *Prog. Inorg. Chem.* **1982**, *29*, 203–283.

[15] a) R. H. Blessing, *Acta Crystallogr., Sect. A* **1995**, *51*, 33–38; b) R. H. Blessing, *J. Appl. Crystallogr.* **1997**, *30*, 421–426.

Received: August 2, 2005
Published Online: December 1, 2005

